Supplementary Information

The Impact of Hydrogen Valence on Its Bonding and Transport in Molten Fluoride Salts

Stephen T. Lam[1,2]*, Qing-Jie Li[1], Jonathan Mailoa[3], Charles Forsberg[1], Ronald Ballinger[1,4], Ju Li[1,4]

[1]Department of Nuclear Science and Engineering, Massachusetts Institute of Technology, Cambridge, MA 02139, USA

[2]Department of Chemical Engineering, University of Massachusetts Lowell, Lowell, MA 01854, USA

[3]Bosch Research and Technology Center, Cambridge, MA 02139, USA

[4]Department of Materials Science and Engineering, Massachusetts Institute of Technology, Cambridge, MA 02139, USA

* Corresponding author: stephen_lam@uml.edu

Supplementary Notes

Supplementary Note 1: Simulated versus experimental local structure of fluorides

For structural analysis, X-ray and neutron diffraction methods are most commonly used. In polyatomic systems, the total interference function $F_N(Q)$ is decomposed into a weighted linear combination of the component pair structure factors $S_{\alpha\beta}(Q)$. Taking Fourier transforms of these structure factors, the real space distribution functions $g_{\alpha\beta}(r)$ are determined. In practice, scattering methods for multi-component systems should be coupled to simulation and other experimental methods to fully understand and resolve features of the diffraction pattern [1][2][3].

The fluoride salts LiF, NaF, KF, BeF_2, Flibe and Flinak are simulated since they are the prototypical salt and salt constituents of interest. The local structure is determined by the radial distribution function and compared. Overall, there is good agreement between the simulations and experiments across a range of fluorides. The radial distribution functions are determined experimentally using X-ray or neutron diffraction and the results are discussed here.

The calculated RDFs for binaries are shown Figure S1. All of them show a distinct solvation shell between the cation and the anion, and no long-range order as would be expected for a molten solution of charged ions. The first-peak radial distances are ordered BeF_2, Li-F, Na-F and K-F from shortest to longest correlating with their respective atomic radii ($r_{Be^{2+}} < r_{Li^+} < r_{Na^+} < r_{K^+}$). For the salts with monovalent cations, the first maximum of the anion-anion and cation-cation functions corresponds to the first minimum of the cation-anion function. This typically indicates the existence of solvation shells of alternating positive and negative charge [4]. Further, the anion-anion and cation-cation functions are similar with minima and maxima located at the same positions, which indicates that the diffraction patterns would have a single characteristic length. In the divalent cation fluoride BeF_2, the first peak of the cation-anion RDF is much sharper, narrower and occur at a shorter distance. This is indicative of a more orderly solvation shell with well-defined coordination. These results agree qualitatively with previous experimental and computational studies of monovalent and multivalent salts. For example, Be^{2+} in BeF_2 has been found to bind to four fluorine atoms, predominately forming BeF_4 tetrahedral complexes, while monovalent salt cations like Li^+ have been found to coordinate between three and six F^- ions [5].

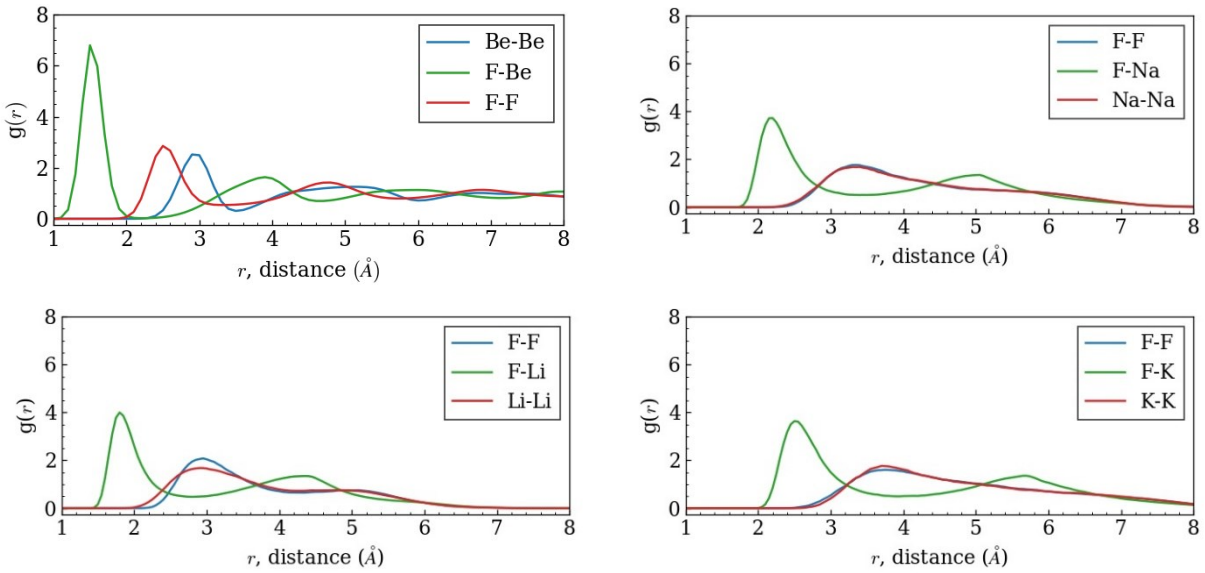

Figure S1: Radial distribution functions (From left to right, top to bottom) for BeF_2, NaF, LiF and KF including cation-anion, anion-anion, and cation-cation pair functions.

The structures of Flibe and Flinak were also examined since they are prototypical salts in many nuclear applications due to their desired thermal hydraulic and neutronic properties [6][7]. The RDFs for Flibe and Flinak are shown in Figure S2. In both the salts, the relative positions of the RDFs are analogous to their constituent binaries shown in Figure S1. For Flibe, the Be-F peak occurs before the Li-F peak and has a higher maximum, just as they were in comparing the binaries. Similarly, the peaks for Li-F, Na-F, and K-F are also ordered by increasing peak distance. Qualitatively, this shows that some of the local chemical behavior of the binary salts is retained when binaries are mixed together.

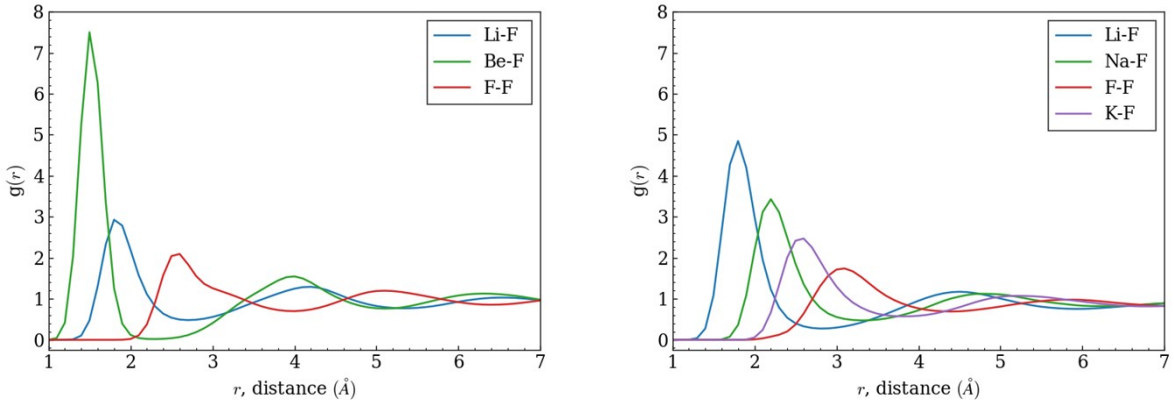

a **b**

Figure S2: Radial distribution functions for a) Flibe at 973K and b) Flinak at 973K.

Table S1. First peak radius and coordination number of various fluorides [8][9][6][7]

Salt	Pair	First Peak Radius (Å)			Coordination Number (N)		
		Experiment	Simulation	|Δ|	Experiment	Simulation	|Δ|
BeF_2	Be-F	1.59	1.5	0.09	4.0	3.75	0.25
	F-F	2.54	2.5	0.04	-	-	-
LiF	Li-F	1.85	1.8	0.05	3.0	2.6	0.4
	F-F	3.0	3.0	0	-	-	-
NaF	Na-F	2.30	2.2	0.1	4.1	3.7	0.4
	F-F	3.5	3.3	0.2	-	-	-
KF	K-F	2.60	2.5	0.1	4.3	4.2	0.1
	F-F	3.9	3.7	0.2	-	-	-
Flibe	Li-F	1.85	1.8	0.05	4.0	4.0	0
	Be-F	1.58	1.5	0.08	4.0	3.7	0.3
	F-F	2.56	2.5	0.06	-	-	-
Flinak	Li-F	1.83	1.8	0.03	3.3	3.6	0.3
	Na-F	2.18	2.2	0.02	3.8	4.9	1.1
	K-F	2.59	2.6	0.01	4.0	6.9	2.9
	F-F	3.05	3.1	0.05	-	-	-

*The experimental temperatures for LiF, NaF, and KF, flibe and flinak were 875, 1000, 870^{o}C, 750^{o}C and 520^{o}C respectively and simulations are controlled to the same temperature.

For all systems, the first peak distances and average coordination number obtained are compared to experimental values in Table S1. In almost all salts pairs, the experimental first peak distance was accurately reproduced within $\pm$ 0.1 Å, which is the width of the bins used to calculate the RDFs. The coordination numbers for the binaries and Flibe were also accurately reproduced with the simulation values within 0.5, indicating accurate representation of the coordination chemistry. In Flinak, the calculated coordination numbers were larger than the experimental values. This can be attributed to the fact that the peaks are broader, and the first minimum is found over a wide and fat tail, with minima ranging from 2.8 – 3.8 Å for cation-anion pairs. Here, small errors in estimating the minimum distance results in large errors in the coordination number, making the calculated numbers meaningless. In all the salts, the small difference can be attributed to small differences in ability to control the experimental and the simulation temperature, numerical approximation in integrating the RDFs, and integration over a weak solvation shell with a poorly defined first minimum. Yet, the structures provide generally good indication that complex structures can be accurately reproduced. Overall, this gives a good indication that the local structure is well reproduced using the simulation methods.

Supplementary Note 2: Simulated versus experimental diffusion

Experimentally, ionic diffusion is typically measured based on electrochemical techniques, capillary diffusion, diffusion through a membrane or using pulsed-gradient nuclear magnetic resonance [10][11][12][13]. The accuracy is dependent on the uncertainties related to the experiments, which are sometimes run over several hours, and require fit to analytical models. The self-diffusion coefficients for ions in LiF-KF, Flibe and Flinak are calculated and compared against experimental data. These results are shown in Figure S3, S4 and S5. The effects of impurities on diffusion in pure Flibe and tritium are shown in Figures S6 and S7.

For LiF-KF, the simulation values for diffusivity and activation energy are very close to the experimental values, within the errors bars for fluorine. In these figures, the error bars represent the 95% confidence interval from taking the average of block diffusivities. For lithium, the diffusivity values are within ± 1 cm^2/s. There is slight underestimation in the simulation relative to experiment, which likely attributed to cumulative uncertainties of both the experimental and computational methods. Sources of uncertainty include control of both the temperature and pressure. The activation energy for lithium was found to be 31.0 ± 2 kJ/mol compared to the experimental value of 33.0 ± 2 kJ/mol. Similarly, the activation energy for fluorine was found to be 33.0 ± 2 kJ/mol compared to the experimental value of 28.0 ± 1 kJ/mol. For potassium, the diffusivity was not experimentally measured and is thus not shown here. In both elements, the margin of error is small compared to other engineering uncertainties.

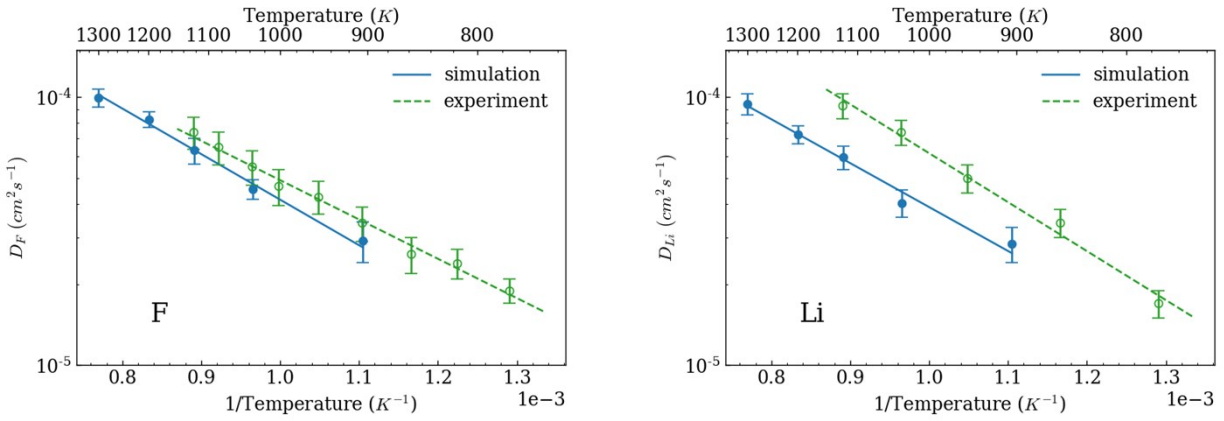

a) b)

Figure S3: Self diffusivity from 775K to 1300K of a) fluorine and b) lithium in eutectic composition of LiF-KF. Experimental data from Sarou-Kainan et al [14].

For Flinak, tracer measurements were conducted by Umesaki and compared against calculations as shown in Figure S4 [15]. The shaded region and error bars represent the 95% confidence interval of the mean estimate. In all cases with Li^+, Na^+, K^+ and F^- ions, the experimental data matched simulations within margin of error in terms of diffusivity values and activation energies. The diffusivities of all ions are very similar despite having different ionic radii. This is due to the coulombic interaction and electronegativity of cations. Even though Li has a smaller radii, the Li^+ interactions with F^- are stronger, therefore decreasing

the effective diffusivity in Flinak. The experimental activation energies for Li, Na, K and F were 37.2 ± 4.2, 36.2 ± 7.1, 32.0 ± 7.5 and 30.8 ± 6.7 kJ/mol respectively, which are effectively the same as the simulation values of 34.0 ± 1, 33.0 ± 3, 35.0 ± 2, and 34.0 ± 2 kJ/mol. These results are comparable to AIMD simulations from Nam et. al in terms of both magnitude of diffusivities and activation energy [16].

The calculated diffusion coefficients in Flibe are shown in Figure S5. The coefficients for Li and F have been measured experimentally by Omichi et. al and Iwamato et. al (Janz database) [17][18]. For Lithium, the average simulation values are lower than the experimental values, although they are close to the lower range of the experiment values. However, the activation energies are similar with the Li simulation value as 32.0 ± 1 kJ/mol compared to experimental value of 32 ± 8.4 kJ/mol. The difference could be related to systematic errors previously noted in simulation and experiment, which seems to cause a slight under prediction of simulation values relative to the experimental as shown in the case of the lithium ion in LiF-KF. Further, Iwamoto showed that lithium diffusion in a 50-50 mixture of LiF-BeF_2 was on the order of 5E-8 m^2/s lower than that lithium in Flibe and similar to the calculated values. As such, a contribution to the total error could be caused by concentration uncertainties.

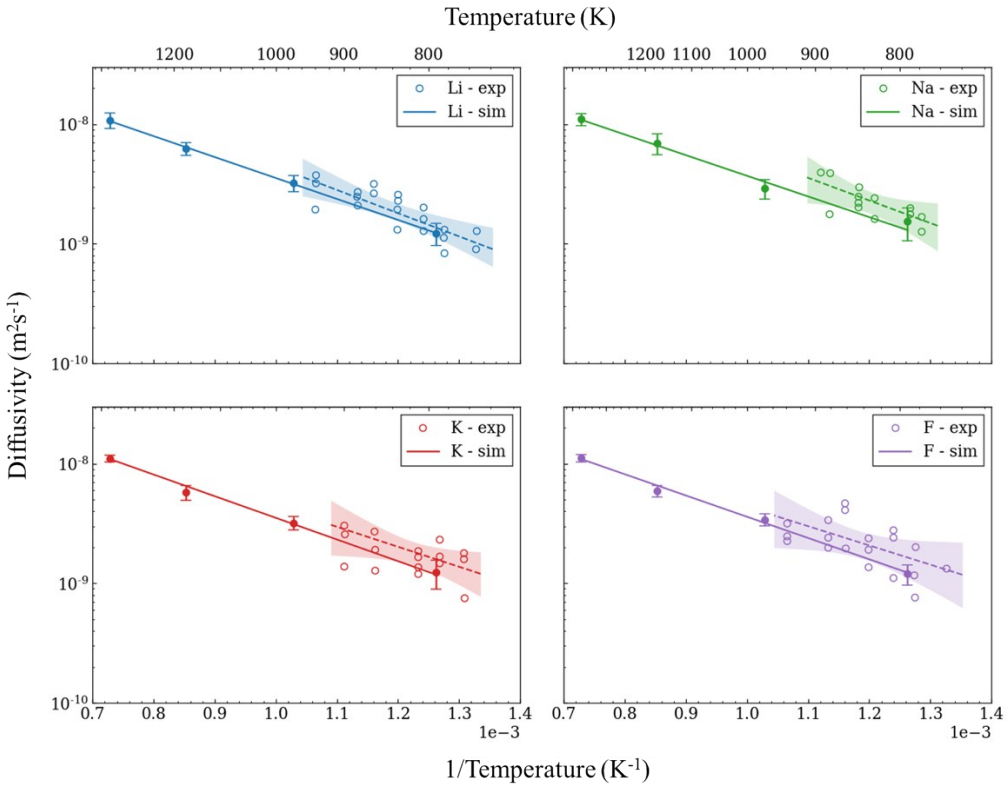

106

107 Figure S4: Self diffusivity of ions in Flinak compared to experimental data [15].

108 For fluorine in Flibe however, the difference cannot be explained by uncertainties alone. The
109 fluorine ion showed much higher diffusivity than the simulation value at 1000K and a much higher
110 activation energy. The simulation activation energy for fluorine was similar to lithium at 30.0 $\pm$ 2.5 kJ/mol,
111 while experimental activation energy was 128 $\pm$ 14 kJ/mol. It is speculated by Ohmichi et. al that fluorine
112 diffuses either by exchange across neighboring beryllium fluoride anions BeF_4^{2-} or by Li-F pairs. However,
113 the high diffusivity and activation energy are not fully explained. Contrary to experimental measurements,
114 the formation of Be-F polymer-like structures should lower average diffusivity since the fluorine is more
115 strongly bound as evidenced by the RDFs in Figure S2.

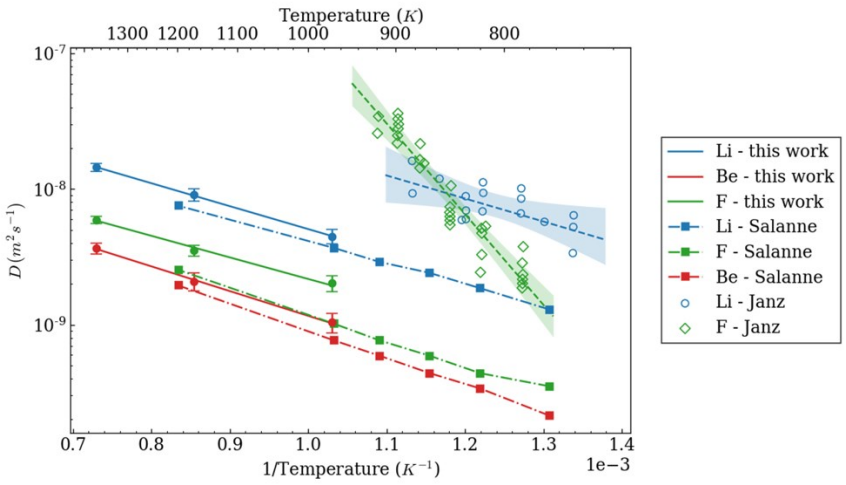

Figure S5: Self diffusivity of Li and F ions in Flibe compared to experiments [10][14].

Since there is only one study on fluorine in Flibe, it is difficult to determine possible experimental errors. The results presented here agree with AIMD and classical MD simulations conducted by Morgan and Salanne [16][19], who calculated similar diffusivities and activation energies as shown in Figure S5. In part, the error could be caused by errors in concentrations of LiF and BeF_2 since BeF_2 is known to form extended BeF_4^{2-} polymer chains at high concentrations. Having a low BeF_2 concentration could liberate fluorine atoms causing the high diffusivity in the experiment. This is tested in Figure S6 a), where for 80-20 LiF-BeF_2 fluorine diffusivity is in fact higher. However, this alone does not explain the high activation energy. Since Flibe is highly hydrophilic with tendency to form BeO when contacted with air, Flibe requires special attention above other fluoride salts [20]. The difference in activation energy suggests a difference in diffusion mechanism between experiments and simulation, which could be caused by changes fluorine complex coordination chemistry due to the presence of impurities. In fact, it has been shown by various experiments that impurity concentration likely dominates corrosion kinetics, which is dependent on both chemical speciation and mass transport [21][22][23][24]. Since Cr is the main corrosion impurity in Flibe, simulations with Flibe and CrF_x are performed as shown in Figure S6 b).

a

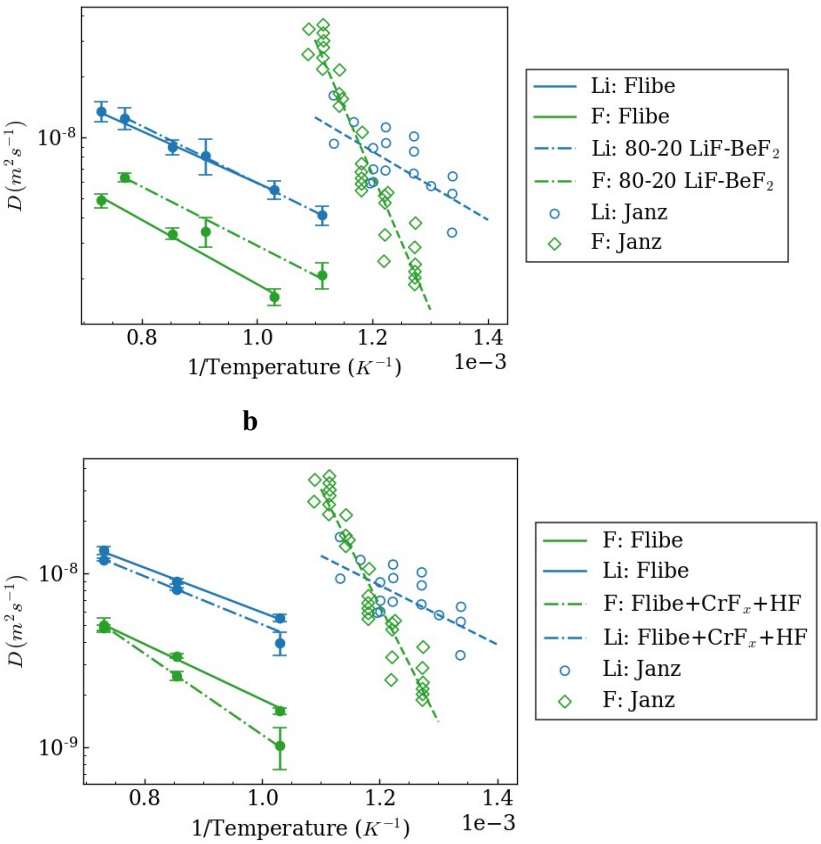

Figure S6: Flibe experiment from Janz database a) 50-50 and 66-33 LiF-BeF_2 simulations. b) Flibe simulation and Flibe with impurities (39 Flibe + 2CrF_3 + CrF_4 + HF).

While the introduction of chromium impurity does not reproduce the experiment result, it does increase the activation energy. It is likely just one of several the factors that are causing to the observed difference between the experiment and our simulations. Given that these simulations succeeded in calculating diffusion coefficients and local structures for ions in Flibe and other similar molten salts, large errors are not expected for solely the fluorine atom. Thus, new experimental studies with Flibe should be conducted.

With respect to tritium diffusivity in Flibe and Flinak, more than an order of magnitude difference was observed across experiments as shown in Figure 5 and 6 in the main text. One possible reason this discrepancy is the presence of impurities in the salt. Impurities have been found previously to significantly increase corrosion rate and could potentially alter other chemically properties [23]. To test this hypothesis, separate simulations were performed for tritium ($^3H^+$) in Flibe introducing a Cr ion and an H_2O molecule. The Cr ion is chosen since it is a common constituent in structural steel and known to corrode most readily

due to the relatively low Gibbs free energy of chromium fluoride. The H_2O molecule is tested since Flibe is known to be hygroscopic and atmospheric moisture could be present in the experiments. When Cr or H_2O was introduced, ^3H diffusivity reduced by up to 25 $\pm$ 10% and 15 $\pm$ 10% respectively relative to tritium diffusivity in clean Flibe. In both cases, this change in diffusivity is attributed to tritium interactions with the impurities in molten salt. $^3H^+$ was found to co-ordinate with the impurity ion forming various coordinated complexes shown in Figure S7.

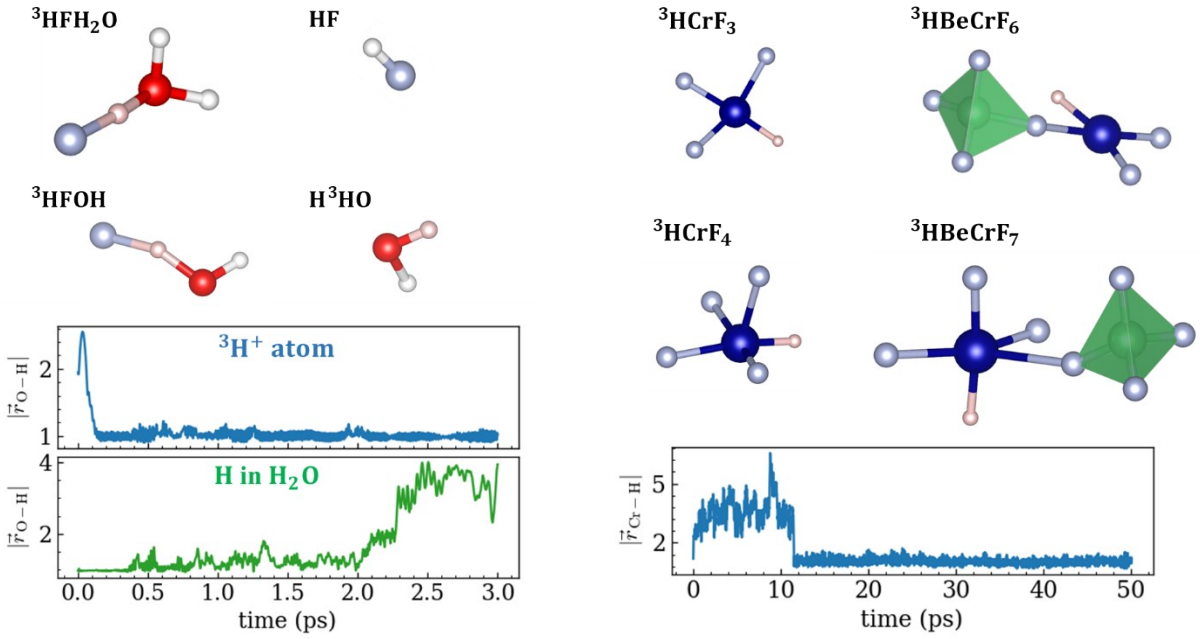

a **b**

Figure S7: **a** Configurations of $^3H^+$ in Flibe with a H_2O molecule. Elements are F (purple), ^3H (pink), H (white), O (red). Plots show 1) top: the distance between $^3H^+$ and oxygen atom, and 2) bottom: H-O distance in the original water molecule. Plots show that the $^3H^+$ will bind to H_2O replacing the original H in the H_2O molecule. **b** Common configurations of $^3H^+$ in Flibe with a Cr atom. Elements are Cr (blue), F (purple), Be (green), and ^3H (pink). Plot shows the interatomic distance between Cr and H, indicating that the $^3H^+$ atom will coordinate to Cr to form various complexes.

When H_2O was introduced, it was found that proton hopping occurred where $^3H^+$ in solution exchanged with the original hydrogen atoms in H_2O. As shown in Figure S7**a**, $^3H^+$ was able to bind to the H_2O forming the intermediate H_2O^3HF and ^3HHO. After 2 ps, one of the original H atoms was ejected and formed HF with surrounding fluorine atoms. The oxygen atom remain bound to the $^3H^+$ ion and the other

H atom for the remainder of the 50 ps simulation. When Cr is introduced into the salt, $^3H^+$ was able to bind to the Cr at 12 ps as shown in Figure 7**b**. The average coordination distance was $\bar{d}_{Cr-H} = 1.7$ Å, and the H remain coordinated with the Cr for the rest of the 50 ps simulation. During this time, several Cr-H coordination complexes were observed including $HCrF_3$ (9 ps), $HCrF_4$ (4.1 ps), $HBeCrF_6$ (2.7 ps), $HBeCrF_7$ (1.5 ps), and other HCrF complexes bound to BeF tetrahedral chains with 2 or more Be atoms. For the most common configuration $HCrF_3$, a planar configuration was observed. This is similar to the planar configuration that was previously found for CrF_4 when Cr was added to Flibe [16], except with the hydrogen atom replacing one of the fluorine atoms. In this previous study, it was found the Cr diffusion rate and fluorine coordination depended on the oxidation state of the Cr. Increasing Cr oxidation state was accompanied by reduced diffusion and increased coordination with fluorine. Thus, Cr oxidation state could potentially have an effect on tritium diffusivity as well. In addition, there are many possible impurities including structural elements and fission products that could be relevant to transport properties, which should be studied in further detail.

References

[1] G. W. Neilson, A. K. Adya, and S. Ansell, "8 Neutron and X-ray diffraction studies on complex liquids," *Annu. Reports Prog. Chem. - Sect. C*, vol. 98, no. 1, pp. 271–320, 2002.

[2] L. B. Skinner *et al.*, "Structure of Molten CaSiO3: Neutron Diffraction Isotope Substitution with Aerodynamic Levitation and Molecular Dynamics Study," *J. Phys. Chem. B*, vol. 116, no. 45, pp. 13439–13447, Nov. 2012.

[3] H. E. Fischer, A. C. Barnes, and P. S. Salmon, "Neutron and x-ray diffraction studies of liquids and glasses," *Reports Prog. Phys.*, vol. 69, no. 1, pp. 233–299, 2006.

[4] M. Salanne, C. Simon, P. Turq, N. Ohtori, and P. A. A. Madden, "Modeling of Molten Salts," in *Molten Salts Chemistry*, 1st ed., no. i, Elsevier Inc., 2013, pp. 1–16.

[5] A. L. Rollet and M. Salanne, "Studies of the local structures of molten metal halides," *Annu. Reports Prog. Chem. - Sect. C*, vol. 107, pp. 88–123, 2011.

[6] D. Ingersoll *et al.*, "Status of preconceptual design of the advanced high-temperature reactor (AHTR)," ORNL/TM-2004/104, 2004.

[7] L. M. Toth, G. D. Del Cul, S. Dai, and D. H. Metcalf, "Molten fluoride fuel salt chemistry," *AIP*

Conf. Proc., vol. 324, no. 1, pp. 1139–1142, 1995.

[8] S. Mukhopadhyay and F. Demmel, "Modelling of structure and dynamics of molten NaF using first principles molecular dynamics," *AIP Conf. Proc.*, vol. 1969, no. May, 2018.

[9] F. Vaslow and A. H. Narten, " Diffraction pattern and structure of molten BeF 2 –LiF solutions ," *J. Chem. Phys.*, vol. 59, no. 9, pp. 4949–4954, 1973.

[10] G. J. Janz and N. P. Bansal, "Molten Salts Data: Diffusion Coefficients in Single and Multi Component Salt Systems," *J. Phys. Chem. Ref. Data*, vol. 11, no. 3, pp. 505–693, 1982.

[11] I. Farnan and J. F. Stebbins, "High-Temperature29Si NMR Investigation of Solid and Molten Silicates," *J. Am. Chem. Soc.*, vol. 112, no. 1, pp. 32–39, 1990.

[12] A. L. Rollet, V. Sarou-Kanian, and C. Bessada, "Measuring self-diffusion coefficients up to 1500 K: A powerful tool to investigate the dynamics and the local structure of inorganic melts," *Inorg. Chem.*, vol. 48, no. 23, pp. 10972–10975, 2009.

[13] C. S. Johnson, "Diffusion ordered nuclear magnetic resonance spectroscopy: Principles and applications," *Prog. Nucl. Magn. Reson. Spectrosc.*, vol. 34, no. 3–4, pp. 203–256, 1999.

[14] V. Sarou-Kanian, A. L. Rollet, M. Salanne, C. Simon, C. Bessada, and P. A. Madden, "Diffusion coefficients and local structure in basic molten fluorides: in situ NMR measurements and molecular dynamics simulations," *Phys. Chem. Chem. Phys.*, vol. 11, no. 48, pp. 11501–11506, 2009.

[15] N. Umesaki, N. Iwamoto, Y. Tsunawaki, H. Ohno, and K. Furukawa, "Self-diffusion of lithium, sodium, potassium and fluorine in a molten LiF + NaF + KF eutectic mixture," *J. Chem. Soc. Faraday Trans. 1 Phys. Chem. Condens. Phases*, vol. 77, no. 1, pp. 169–175, 1981.

[16] H. O. Nam, A. Bengtson, K. Vörtler, S. Saha, R. Sakidja, and D. Morgan, "First-principles molecular dynamics modeling of the molten fluoride salt with Cr solute," *J. Nucl. Mater.*, vol. 449, no. 1–3, pp. 148–157, 2014.

[17] T. Ohmichi, H. Ohno, and K. Furukawa, "Self-diffusion of fluorine in molten dilithium tetrafluoroberyllate," *J. Phys. Chem.*, vol. 80, no. 14, pp. 1628–1631, 1976.

[18] N. Iwamoto, Y. Tsunawaki, N. Umesaki, H. Ohno, K. Farukawa, and K. Furukawa, "Self-diffusion of lithium in molten LiBeF3 and Li2BeF4," *J. Chem. Soc. Faraday Trans. 2 Mol. Chem. Phys.*, pp. 1277–1283, 1978.

[19] R. J. Heaton, R. Brookes, P. A. Madden, M. Salanne, C. Simon, and P. Turq, "A First-Principles Description of Liquid BeF2 and Its Mixtures with LiF: 1. Potential Development and Pure BeF2," *J. Phys. Chem. B*, vol. 110, no. 23, pp. 11454–11460, 2006.

[20] M. S. Sohal, M. a Ebner, P. Sabharwall, and P. Sharpe, "Engineering database of liquid salt thermophysical and thermochemical properties," Idaho National Laboratory, Idaho Falls, Idaho, INL/EXT-10-18297, 2013.

[21] J. Zhang *et al.*, "Redox potential control in molten salt systems for corrosion mitigation," *Corros. Sci.*, vol. 144, pp. 44–53, 2018.

[22] S. Guo, J. Zhang, W. Wu, and W. Zhou, "Corrosion in the molten fluoride and chloride salts and materials development for nuclear applications," *Prog. Mater. Sci.*, vol. 97, pp. 448–487, 2018.

[23] J. Zhang, "Impurities in Primary Coolant Salt of FHRs: Chemistry, Impact, and Removal Methods," *Energy Technol.*, vol. 7, no. 10, pp. 1–13, 2019.

[24] Y. Wang, S. Zhang, X. Ji, P. Wang, and W. Li, "Material corrosion in molten fluoride salts," *Int. J. Electrochem. Sci.*, vol. 13, no. 5, pp. 4891–4900, 2018.